From Concentration Profiles to Polymer Osmotic Equations of State

Chris I. Addison,* Jean-Pierre Hansen, and Ard A. Louis[a]

While the osmotic equation of state (e.o.s.) of off-lattice models of polymer solutions or melts can be readily computed from the contact theorem, according to which the osmotic pressure is proportional to the monomer density at a hard wall,[1] the task is significantly more arduous for polymers on a lattice. For short chains or low polymer concentrations, the chemical potential may be calculated from the insertion probability of a test chain[2] and the pressure then follows by standard thermodynamic integration. The insertion method can be extended to solutions of longer polymers provided configurational bias Monte Carlo (MC) algorithms are used.[3,4] An alternative method, the repulsive wall thermodynamic integration (RWTI) method, which remains efficient at high polymer concentrations, or in the melt, was proposed by Dickman.[5] It extends the contact-theorem approach but requires several simulation runs for increasing wall–monomer repulsion and subsequent thermodynamic integration for each state point, rendering the method rather cumbersome. Moreover, a recent analysis by Stukan et al.[6] revealed that the RWTI method is prone to large finite-size effects, particularly at high polymer concentrations, which can only be overcome by switching to grand-canonical ensemble simulations.

Herein, we show that the e.o.s. of dilute or semidilute polymer solutions is much more efficiently computed by subjecting the polymers to a strong gravitational field. The resulting sedimentation profile of the polymer solution then leads directly, via the hydrostatic equilibrium condition, to the osmotic e.o.s. over a wide range of concentrations from a single MC run. The method extends an idea which has been successfully applied to concentrated dispersions of rigid colloidal particles (e.g., spherical[7,9] or platelike[8]) to the case of flexible polymers; it applies to on- and off-lattice models alike.

Sedimentation equilibrium of macromolecular solutions or colloidal dispersions arises from the balance between gravity, which pulls particles to lower altitudes z, and the entropic drive toward homogeneity, and is characterised by a concentration profile $\rho(z)$. If m is the buoyant mass of the particles, the sedimentation length is defined by $\zeta = k_B T/mg$, where g is the acceleration of gravity and $k_B T$ the thermal energy. For compact, micron-sized colloids, ζ is typically of the order of a few particle diameters, but for the much lighter fractal polymer chains, ζ is very large under normal gravity, so that the solution remains nearly homogeneous in practice. However, in simulations g can be tuned to induce a measurable modulation of the concentration profile.

[a] C. I. Addison, Prof. J.-P. Hansen, Dr. A. A. Louis
Department of Chemistry, University of Cambridge, (United Kingdom)
Fax: (+44) 1223-336-362
E-mail: cia21@cam.ac.uk

  DOI: 10.1002/cphc.200400524

We consider systems of N polymer chains, each of L monomers (or segments) living on a cubic lattice of spacing a. Each site hosts at most one monomer, corresponding to the self-avoiding-walk (SAW) model, while non-connected nearest-neighbour segments interact with energy $-\varepsilon$. The dimensionless inverse temperature is $\beta^* = \beta\varepsilon = \varepsilon/k_BT$; $\beta^* = 0$ corresponds to the athermal SAW limit, while the θ-solvent regime is reached for $\beta^* \approx 0.265$ for $L = 500$ chains.[10] Each monomer experiences the gravitational energy $-mgz$, and the gravitational coupling constant is the dimensionless ratio $\lambda_m = a/\zeta_m = mga/k_BT$. Sedimentation equilibrium is characterised by the monomer concentration profile $\rho_m(z)$, that is, the mean number of monomers per unit volume at altitude z. A more coarse-grained representation focuses on the centre of mass (CM) of each polymer coil, of characteristic dimension equal to the radius of gyration R_g. The gravitational field acts on the CM, and the corresponding sedimentation length is $\zeta_{cm} = k_BT/Mg = \zeta_m/L$ where $M = Lm$ is the total mass of the polymer. The relevant gravitational coupling constant is given by Equation (1):

$$\lambda_{cm} = \frac{R_g}{\zeta_{cm}} = \frac{MgR_g}{k_BT} = \lambda_m L \frac{R_g}{a} \sim \lambda_m L^{1+\nu} \quad (1)$$

where $R_g \sim aL^\nu$ with ν the Flory exponent ($\nu \approx 0.59$ in good solvent and $\nu = 0.5$ in θ solvent). At sedimentation equilibrium, the CM concentration profile is $\rho_{cm}(z)$, which satisfies the normalisation, Equation (2):

$$\int_0^\infty \rho_{cm}(z)\mathrm{d}z = n_s \quad (2)$$

where $n_s = N/A$ is the number of polymers per unit area of an x–y cross-section of the sedimentation column.

Two limits of the concentration profile are known explicitly. First, the system of independent (free) monomers, that is, $L = 1$ polymers, reduces in the SAW limit ($\beta^* = 0$) to a single-occupancy lattice gas in a gravitational field. The corresponding concentration profile $\rho_m^{(i)}$ is easily calculated by Equation (3):

$$\rho_m^{(i)}(z) = \frac{e^{\beta\mu - z/\zeta_m}}{1 + e^{\beta\mu - z/\zeta_m}} \quad (3)$$

where μ is the monomer chemical potential. At sufficiently high altitudes ($z \to \infty$) the profile follows the barometric law for monomers: $\rho_m^{(i)}(z) \sim \exp(-\beta mgz) \sim \exp(-z/\zeta_m)$. Upon introducing connectivity constraints, however, the concentration profile contracts significantly. At high altitudes z, where the polymer–polymer interactions are negligible, the concentration profile takes the form of Equation (4):

$$\rho_m(z) \propto \rho_{cm}(z) \sim \exp(-\beta mLgz) \sim \exp(-z/\zeta_{cm}) \quad (4)$$

following the barometric law for polymers. In other words, it is contracted by a factor L over a system of unconnected monomers. This follows from the well-known $1/L$ reduction of the ideal component of the osmotic pressure of polymer solutions $P^{id} = \rho_m/L$, where ρ_m is the bulk monomer concentration. In fact, if the e.o.s. and, hence, the free-energy density of a homogeneous ($g = 0$) polymer solution is known as a function of bulk polymer concentration ρ and temperature, the full concentration profile in the weak-modulation limit $\lambda \ll 1$ can be easily calculated within the local density approximation (LDA).[7] Herein, we adopt the opposite point of view. We solve the inverse problem and, as explained further in this Communication, we extract the unknown e.o.s. from concentration profiles computed by MC simulations.

The simulations were carried out for the cubic lattice model defined earlier, in a simulation box of dimensions $l_x \times l_y \times l_z$ in units of a. The square base of area $A = l_x \times l_y$ was periodically repeated in the x and y directions; most runs were for $l_x = l_y = 100$. The vertical dimension l_z was chosen such that for reasonable values of the gravitational coupling constant λ_{cm}, the polymer concentration at the highest altitude was negligible compared to that at the bottom. Most simulations were carried out for $N = 1600$ polymers of length $L = 500$ by using pivot, translation, reptation, and configurational bias MC moves.[4] Starting from an initial homogeneous configuration, the system was equilibrated until the downward drift of the overall CM of the system stopped. The profiles $\rho_m(z)$ and $\rho_{cm}(z)$ were then calculated from altitude histograms averaged over several million configurations (the statistics are of course L times better for the monomer than for the CM profiles). For given N, L, and β^*, simulations were carried out for several gravitational couplings λ_{cm}. Local polymer concentrations $\rho_{cm}(z)$ are expressed relative to the bulk overlap concentration $\rho^* = 3/4\pi R_g^3$ where R_g is chosen to be the temperature-dependent radius of gyration at zero concentration. For a given N, higher values of λ_{cm} are required to achieve higher polymer concentrations near the bottom of the simulation cell.

Examples of concentration profiles $\rho_m(z)$ and $\rho_{cm}(z)$ for $\beta^* = 0$, a model for polymers in a good solvent, are shown in Figure 1. As expected, the profiles steepen when gravity, that is, λ_{cm} increases. The CM profiles exhibit a marked first adsorption layer at the bottom, which is much smaller in $\rho_m(z)$ profiles,[11] but beyond that layer the two profiles coincide within

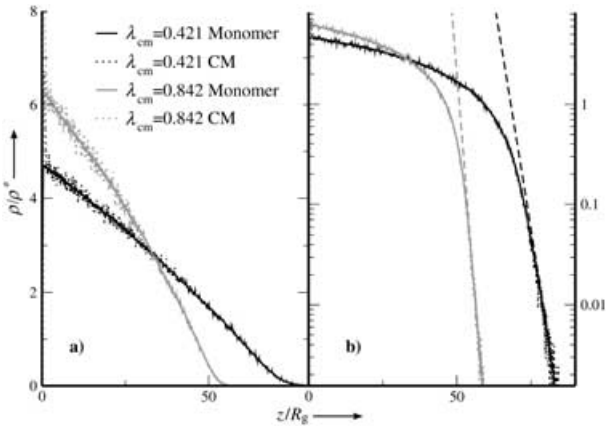

Figure 1. Monomer and CM profiles for $N = 1600$ SAW polymer chains of length $L = 500$, shown for two values of the gravitational coupling constant λ_{cm}. a) Profiles plotted on a linear scale. b) The same profiles but now plotted on a logarithmic scale. The dashed lines denote the barometric law [Eq. (4)] valid at low densities.

the statistical errors of $\rho_{cm}(z)$. The CM layering and preceding "correlation hole" in $\rho_{cm}(z)$ (which is more clearly apparent in Figure 2) may be traced back to the effective wall/CM repul-

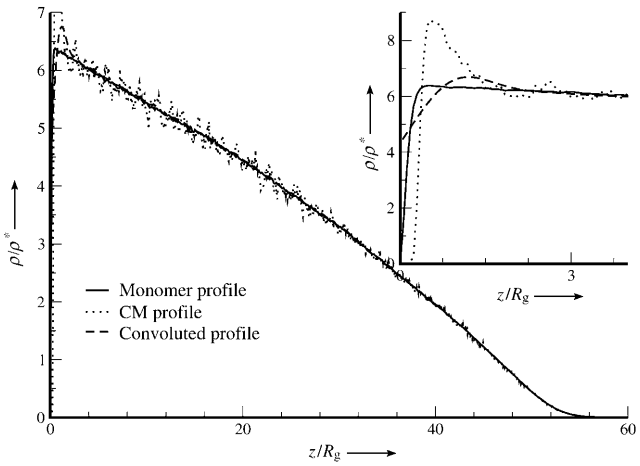

Figure 2. Concentration profiles for $N=1600$ polymers of length $L=500$, at $\lambda_{cm}=0.842$ and $\beta^*=0$. The dashed line is the convoluted profiles obtained from Equation (6).

sion of entropic origin.[11] The logarithmic plots of the profiles reveal linear behaviour at high altitudes with slopes of $-1/\zeta_{cm}$, in agreement with the asymptotic barometric behaviour, thus providing a direct check on the convergence of the MC simulations. The close agreement between $\rho_m(z)$ and $\rho_{cm}(z)$ beyond the CM adsorption layer is of course a consequence of the polymer connectivity. The agreement may be quantified by assuming that the monomer/CM form factor (which describes the distribution of monomers around the CM in a polymer coil) is independent of the local polymer density and taken to be that appropriate for an ideal (Gaussian coil) polymer, namely, Equation (5):

$$\omega_{cm}(r) = \frac{L}{R_g^3} e^{(-3r^2/2R_g^2)} \tag{5}$$

where $r^2=x^2+y^2+z^2$ is the monomer/CM distance squared. The approximate relation between $\rho_m(z)$ and $\rho_{cm}(z)$ is then simply given by the following convolution in Equation (6):

$$\rho_m(z) = \int_0^\infty \omega_{cm}(|z-z'|)\rho_{cm}(z')dz' \tag{6}$$

An example is shown in Figure 2. The agreement between the "exact" $\rho_m(z)$ and the approximation is seen to be good, except at distances less than R_g from the wall where the internal structure of the polymers is expected to be distorted compared to its bulk behaviour.

Concentration profiles $\rho_m(z)$ and $\rho_{cm}(z)$ under θ-solvent conditions ($\beta^*=0.265$) are shown in Figure 3 for two gravitational couplings λ_{cm}. The logarithmic plots show that the profiles reach the asymptotic barometric law earlier than in the SAW

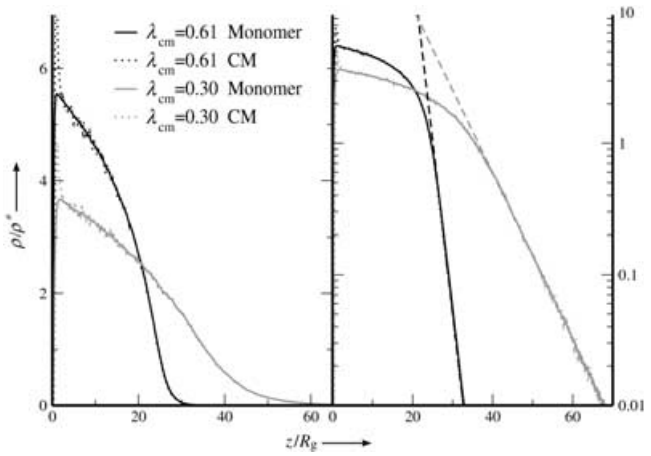

Figure 3. θ-solvent monomer and CM concentration profiles. In the dilute regime, the θ-solvent e.o.s. resembles that of ideal polymers, and so follows the barometric law up to higher densities than polymers in a good solvent do.

case, but begin to show important deviations from the asymptotic limiting law of Equation (4) at $\rho \gtrsim \rho^*$. In other words, polymers behave ideally in a θ solvent in the dilute regime $\rho < \rho^*$ only.[12]

To extract an osmotic e.o.s. from a concentration profile, we proceed as in ref. [7]. For sufficiently slowly varying profiles, that is, for sufficiently weak external field, the LDA holds and the Euler–Lagrange equation associated with the minimisation of the free-energy functional with respect to the concentration profile $\rho_{cm}(z)$ leads back to the macroscopic equation of hydrostatic equilibrium, Equation (7):[7]

$$\frac{dP(z)}{dz} = -Mg\rho_{cm}(z) \tag{7}$$

where $P(z)$ is the local osmotic pressure at altitude z. Integration of Equation (7) yields Equation (8):

$$\beta P(z) = \frac{1}{\zeta_{cm}} \int_z^\infty \rho_{cm}(z')dz' \tag{8}$$

Thus, $P(z)$ and $\rho_{cm}(z)$ are known as functions of altitude, with elimination of z leading to the desired e.o.s. of the bulk polymer solution $P=P(\rho_{cm},T)$. Note that the LDA approximation is not expected to be accurate near the hard wall where $\rho_{cm}(z)$ varies rapidly within the first adsorption layer, so that the lower integration limit in Equation (8) should be taken at $z \gtrsim R_g$, that is, beyond the peak of $\rho_{cm}(z)$, where $\rho_{cm}(z)$ and $\rho_m(z)$ become indistinguishable.

Equation (8) has an obvious intuitive interpretation: the system relaxes to a density $\rho(z)$ such that the local pressure $P(\rho(z))$ counteracts the weight of the polymers above. Conversely, when the e.o.s. is known, Equation (7) can be directly integrated to calculate the concentration profile;[7] for example, in the semidilute regime, where the osmotic equation of state obeys the well-known scaling law $\beta P(\rho)/\rho \sim \gamma(\rho/\rho^*)^{1/(3\nu-1)}$,[13] with γ a dimensionless constant that depends on polymer de-

tails, the resulting concentration profile is given by Equation (9):

$$\rho^{sd}(z) = \rho_0 \left[1 - \left(\frac{\rho_0}{\rho^*}\right)^{\frac{1}{1-3\nu}} \frac{\lambda_{cm}}{3\gamma\nu} \frac{z}{R_g}\right]^{3\nu-1} \quad (9)$$

where ρ_0 is the maximum polymer density, reached at $z=0$, and follows from inverting Equation (10):

$$P(\rho_0) = Mgn_s \quad (10)$$

if the wall-induced layering at the bottom of the container is ignored. Equation (9) provides an accurate fit to the density profile in the semidilute regime, but at higher altitude the analytic profile $\rho(z)$ fails to cross over to the barometric law as illustrated in Figure 4.

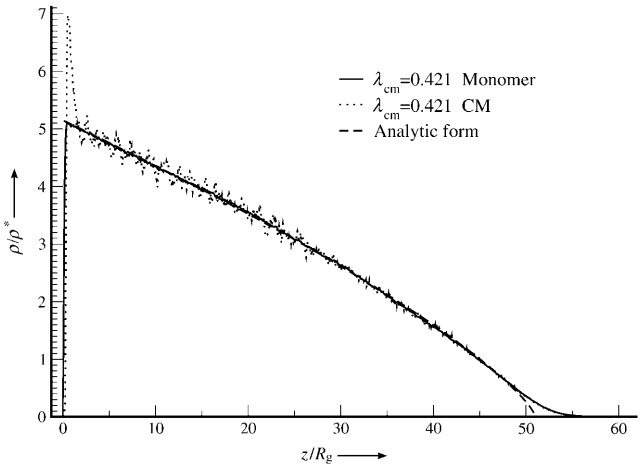

Figure 4. Concentration profiles, compared to the analytic form from Equation (9). Note the excellent agreement in the semidilute regime and the expected disagreement in the dilute regime where the barometric law takes over.

We have carried out the above inversion procedure for $\beta^*=$ 0, 0.1, 0.2, and 0.265 (θ solvent). The resulting e.o.s. $P(\rho,T)$ should be independent of the gravitational coupling used in the MC simulations, provided λ_{cm} is not too large, that is, the gravitational field is not too strong. This was checked explicitly by carrying out the inversion procedure for two different values of λ_{cm}; the resulting e.o.s. always turned out to be practically identical, with very small differences (typically less than 1% over the whole concentration range), providing an estimate for the sum of systematic and statistical errors. However, if the applied gravitational field is too strong ($\lambda_{cm} \gtrsim 1$), the resulting profiles vary too rapidly with z for LDA to remain accurate. This reflects itself in the failure of the resulting compressibility factor $Z=\beta P/\rho$ to go over to its ideal-gas limit as $\rho\to 0$, as illustrated in the inset of Figure 5. Our results for $Z(\rho,T)$ are plotted in Figure 5, along four isotherms, and compared to the predictions of MC simulations of bulk polymer solutions[12] based on the RWTI procedure.[5] The agreement is seen to be excellent throughout. In fact, some apparent discrepancies be-

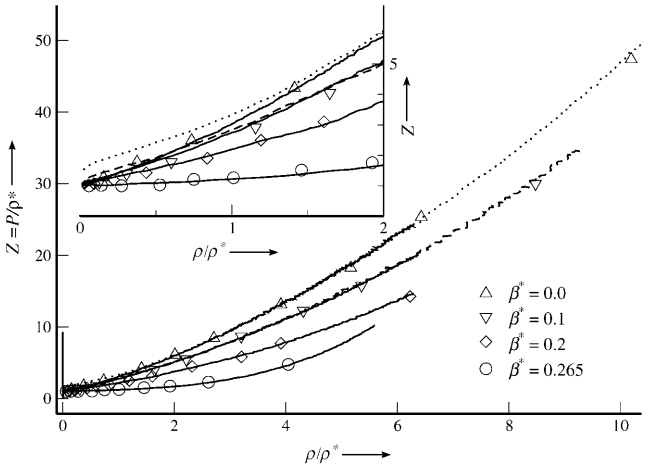

Figure 5. Equation-of-state isotherms calculated by inversion of concentration profiles (lines) compared to those of earlier simulations[12] using the RWTI method (symbols). Whereas the former need about 50 independent simulations per isotherm, the method used herein requires only one simulation per isotherm. The solid lines are for runs $\lambda_{cm}<1$, the dotted $\beta^*=0$ line is at $\lambda_{cm}=4.21$ and the dashed $\beta^*=0.1$ line is at $\lambda_{cm}=1.97$.

tween our earlier data[12] based on the RWTI method and those obtained with the present method were resolved when contentious RWTI high-concentration points were rerun with considerably improved statistics.

In an effort to detect possible finite-size effects, we repeated some of the simulations with a four-times-larger base area. Any observed differences in the resulting data were within statistical noise.

A related consistency test of the LDA-based inversion procedure is provided by the scale-invariance property of the LDA concentration profile, according to which, along any isotherm, the rescaled profiles $\rho_{cm}(z/\zeta_{cm})$ or $\rho_m(z/\zeta_{cm})$ depend only on the dimensionless product $n_s\lambda_{cm}a^2$. This means that as long as LDA applies, the rescaled profiles should be identical if the number of polymers is divided by a given factor, provided the gravitational coupling λ_c is multiplied by the same factor. An illustration of this scale invariance is shown in Figure 6. The equations of state extracted from the density profiles are in perfect agreement. Deviations from scale invariance would signal the breakdown of the LDA assumption, providing a diagnostic for the consistency of the procedure.

By inverting the concentration profile in an imposed external field, we measure the full equation of state in a single simulation. This contrasts with the RWTI method,[5] where for each value of ρ a number of separate simulations are needed to perform thermodynamic integration; for example, when we calculated the e.o.s. of $L=500$ polymers as a function of solvent quality in ref. [12], using the RWTI method, we needed about five simulations for each of the ten state points along each isotherm. Herein, we used only one simulation of similar size to each of the 50 simulations per isotherm carried out in ref. [12]. As demonstrated in Figure 5, the results are of comparable accuracy, but achieved with considerably less CPU time.

For a given λ_{cm} and number of polymers N, the maximum density achieved under an external field can be estimated

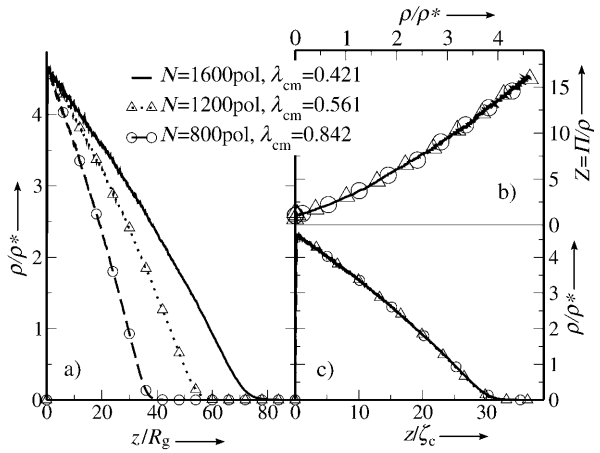

Figure 6. a) Three different concentration profiles from simulations with different numbers of polymers and gravitational strengths, but with the product $n_s\lambda_{cm}a^2$ held constant. Note that b) the equations of state generated from the concentration profiles are practically identical, as are c) the concentration profiles when scaled by the gravitational length.

from Equation (10). If the e.o.s. scales as $\beta P(\rho)R_g^3 \sim (\rho/\rho^*)^\alpha$, then the maximum density ρ_0 scales as shown in Equation (11):

$$(\rho_0/\rho^*) \propto \left(\frac{N\lambda_{cm}}{A/R_g^2}\right)^{\frac{1}{\alpha}} \qquad (11)$$

Larger ρ_0 can be achieved by increasing λ_{cm}, although this is constrained by the LDA criterion, or by increasing N. For semidilute polymers $\alpha \approx 2.3$ in a good solvent and $\alpha \approx 3$ in a θ solvent.[12,13] To double ρ_0, the number of polymers N must be increased by a factor of five for the former—and of eight for the latter—solvent quality. On the other hand, for the RWTI method, doubling ρ_0 simply means doubling N, irrespective of α. Of course to calculate an isotherm, this may also imply doubling the number of different ρ at which independent simulations must be performed. Furthermore, as pointed out by Stukan et al.,[6] finite-size effects become more severe for larger polymer concentrations. As an example, they calculated the pressure of bond-fluctuation model polymers of length $L=20$, using a box with a width $l_x=l_y=20$ and varying the distance l_z between the two hard walls used for thermodynamic integration. At the rather high monomer packing fraction $\phi=NL/V=0.5$ they used, the influence of the two hard walls was noticeable even up to distances of $l_z=160$, where the RWTI method overestimated the pressure by about 3%. We performed comparable simulations for $L=20$ SAW polymers at the same melt-like density. In a gravitational field, we were able to reproduce the $l_z\to\infty$ results of the RWTI method, but with the number of polymers N which the latter method would need for a size $l_z=20$ box only. Thus the less favourable scaling of our external-field method with N is partially offset by less severe finite-size effects, allowing significantly fewer particles to be used.

We have shown that the hydrostatic equilibrium method, which allows the e.o.s. of polymer solutions to be computed along an isotherm in a single simulation, which determines the polymer concentration profiles in a gravitational field, is both accurate and efficient. It provides the osmotic pressure as a function of concentration with a computational effort which is a small fraction (typically under 5%) of that required by using the RWTI method, since the latter requires a series of MC simulations at different densities, and several independent simulations at each density are needed for thermodynamic integration. Moreover, the finite-size problems which can affect the RWTI method are insignificant in the present method, mainly because the simulated system is "open" at high altitudes, that is, essentially extends to infinity in the z direction. The hydrostatic equilibrium method applies equally well to on- and off-lattice models of interacting polymers. The only apparent limitation of the method is that a large gravitational field, that is, large values of λ_{cm} are required to achieve large densities. For too large λ_{cm}, the underlying LDA becomes inaccurate, and the inversion procedure can lead to erroneous results. Hence, the method is expected to be well adapted to dilute and semidilute solutions, while to reach polymer densities typical of polymers melts, several runs with increasing values of λ_{cm} are needed to cover successive and partially overlapping ranges of ρ/ρ^*.

We plan to extend the method presented herein to determine the osmotic e.o.s. of more complex polymeric systems, including block copolymer solutions and melts.

Acknowledgements

CIA would like to thank the EPSRC for funding, AAL is grateful for the support of the Royal Society (London).

Keywords: equation of state · Monte Carlo simulations · polymers · theoretical chemistry

[1] J. K. Percus, *J. Stat. Phys.* **1976**, *15*, 505.
[2] A. Bellemans, E. Devos, *J. Polym. Sci. Polym. Symp.* **1973**, *42*, 1195; R. Dickman, C. K. Hall, *J. Chem. Phys.* **1986**, *85*, 3023.
[3] J. I. Siepmann, I. R. McDonald, D. Frenkel, *J. Phys. Condens. Matter* **1992**, *4*, 679.
[4] D. Frenkel, B. Smit, *Understanding Molecular Simulation, 2nd Ed.*, Academic Press, New York, **1996**.
[5] R. Dickman, *J. Chem. Phys.* **1987**, *87*, 2246.
[6] M. R. Stukan, V. A. Ivanov, M. Müller, W. Paul, K. Binder, *J. Chem. Phys.* **2002**, *117*, 9934.
[7] T. Biben, J. P. Hansen, J. L. Barrat, *J. Chem. Phys.* **1993**, *98*, 7330.
[8] M. Dijkstra, J. P. Hansen, P. A. Madden, *Phys. Rev. E* **1997**, *55*, 3044.
[9] R. Piazza, T. Bellini, V. Degiorgio, *Phys. Rev. Lett.* **1993**, *71*, 4267.
[10] P. Grassberger, R. Hegger, *J. Chem. Phys.* **1995**, *102*, 6881.
[11] P. G. Bolhuis, A. A. Louis, J. P. Hansen, E. J. Meijer, *J. Chem. Phys.* **2001**, *114*, 4296.
[12] C. I. Addison, A. A. Louis, J. P. Hansen, *J. Chem. Phys.* **2004**, *121*, 612.
[13] R. H. Colby, M. Rubinstein, *Polymer Physics*, Oxford University Press, Oxford, **2003**.

Received: November 4, 2004
Published online on August 5, 2005

